34th Annual International Conference of the IEEE EMBS
San Diego, California USA, 28 August - 1 September, 2012

Decoding of Finger, Hand and Arm Kinematics Using Switching Linear Dynamical Systems With Pre-Motor Cortical Ensembles

Xiaoxu Kang, *Student Member*, *IEEE*, Marc H. Schieber, and Nitish V. Thakor, *Fellow, IEEE*

***Abstract*— Previous works in Brain-Machine Interfaces (BMI) have mostly used a single Kalman filter decoder for deriving continuous kinematics in the complete execution of behavioral tasks. A linear dynamical system may not be able to generalize the sequence whose dynamics changes over time. Examples of such data include human motion such as walking, running, and dancing each of which exhibit complex constantly evolving dynamics. Switching linear dynamical systems (S-LDSs) are powerful models capable of describing a physical process governed by state equations that switch from time to time. The present work demonstrates the motion-state-dependent adaptive decoding of hand and arm kinematics in four different behavioral tasks. Single-unit neural activities were recorded from cortical ensembles in the ventral and dorsal premotor (PMv and PMd) areas of a trained rhesus monkey during four different reach-to-grasp tasks. We constructed S-LDSs for decoding of continuous hand and arm kinematics based on different epochs of the experiments, namely, baseline, pre-movement planning, movement, and final fixation. Average decoding accuracies as high as 89.9%, 88.6%, 89.8%, 89.4%, were achieved for motion-state-dependent decoding across four different behavioral tasks, respectively (p<0.05); these results are higher than previous works using a single Kalman filter (accuracy: 0.83). These results demonstrate that the adaptive decoding approach, or motion-state-dependent decoding, may have a larger descriptive capability than the decoding approach using a single decoder. This is a critical step towards the development of a BMI for adaptive neural control of a clinically viable prosthesis.**

I. Introduction

Recent advancements in brain–machine interface (BMI) technology have demonstrated that the neural activity of primary motor (M1) cortical ensemble can be used to control the position of an external device [1-7] or to decode the continuous motor kinematics of primates during instructed tasks [8-14]. Traditionally motor control has been hierarchically characterized as premotor cortical neurons, including ventral and dorsal premotor (PMv and PMd), mainly representing the planning and movement selection while M1 neurons controlling the execution of continuous limb trajectories [14]. A few studies have shown that M1 neuronal ensemble has better decoding accuracy for arm, finger or arm kinematics [4, 15]. However, based on our recordings in PMd and PMv cortices using multiple chronically implanted multi-electrode microarrays in a behaving monkey, we demonstrate that PM ensembles can reconstruct continuous finger, hand and arm kinematics with accuracy that is comparable to that of M1 ensembles. This association suggests that a general purpose BMI can employ multiple cortical areas for motor control. Studies have shown that PM neural signals have stable relationship with kinematics data [16]. This opens up the opportunity of motor control using PM ensembles.

Previous studies all tried to decode a complete complex behavior task use a single Kalman filter [10, 13]. However, the kinematics in most behavior tasks change over time, which a single Kalman filter may fail to capture. Therefore, we developed switching linear dynamical systems (S-LDSs) decoder as a principled framework for adaptive decoding based on different epochs, namely, baseline, pre-movement planning phase, movement phase, and final fixation. We demonstrate that S-LDSs can model well the changing dynamics of reach-to-grasp tasks using cortical ensembles from PMv and PMd. The descriptive power of S-LDSs can potentially widely employed for general adaptive neural decoding of motor kinematics.

II. Methods

A. Experiment Setup

One male rhesus monkeys (Macaca mulatta) sat in a polycarbonate primate chair that restrained the neck, torso and legs. It was trained, using its right upper extremity, to follow different visual cues to manipulate, grasp, and reach towards one of four peripheral objects - sphere, perpendicular mounted cylinder (mallet), pushbutton (push), or peripheral coaxial cylinder (pull) - arranged in a planar circle at 60º intervals (Fig. 1). All studies have been approved by the University of Rochester Institutional Animal Care and Use Committee.

Each trial has four epochs (Fig. 2). In the first epoch, the monkey held a home cylindrical object (home object) for a period of 230 to 1130 ms. The second epoch started with the illumination of a blue LED next to one peripheral object. The third epoch began with the onset of the monkey's movements to reach toward the instructed peripheral object. The illumination of a green LED next to the instructed object marked the beginning of the fourth epoch. The monkey held

This work was sponsored in part the DARPA REPAIR program, contract 19GM-1088724; NIH R01 NS040596-09S1.

X. Kang is with the Department of Biomedical Engineering at The Johns Hopkins University, Baltimore, MD. (corresponding author. Email: xkang2@jhu.edu. Phone: 603-923-9512)

N.V. Thakor is with the Department of Biomedical Engineering at The Johns Hopkins University, Baltimore, MD. (Email: nitish@jhu.edu)

M.H. Schieber is with the Department of Neurology, Neurobiology, and Anatomy at the University of Rochester Medical Center, Rochester, NY.

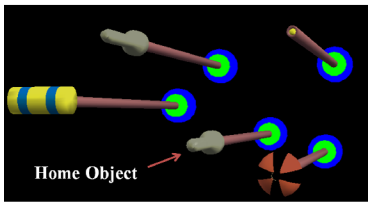

(a)

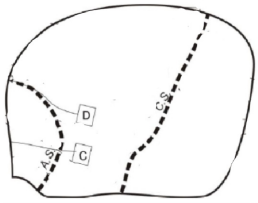

(b)

Figure 1 Experimental Setup. (a) The home object and four peripheral objects. (b) The locations of floating microelectrode arrays (rectangles) implanted in monkey X, traced from intraoperative photographs, relative to two sulci (dashed lines): C.S. - central sulcus, A.S. - arcuate sulcus. Letters C and D designate individual arrays.

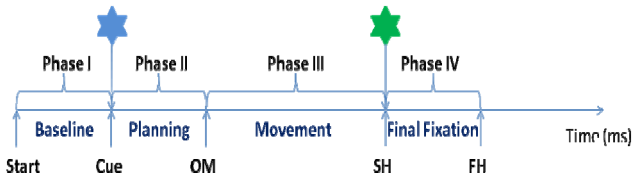

Fig. 2. Timeline of a single trial. The trial is divided into four phases based on the visual cues provided to the monkey during the experiments. Here "start" means the start of the experimental trial; "Cue" indicates the illumination of the blue LED near an instructed object; "OM" refers to the onset of movement of the monkey; "SH" indicates the illumination of the green LED; "FH" refers to the ending signal of the experimental trial, namely, turning off the blue LED.

the instruct peripheral object until a blue LED was turned off to indicate the end of the trial. A detailed description of experimental protocol can be found in [10, 11].

Single-unit activity was recorded using a Plexon (Dallas, TX) data acquisition system from two floating microelectrode arrays (FMA): one in PMd (n=41) and the other in PMv (n=39) respectively. Each FMA includes 16 electrodes and up to four single-units can be discriminated per electrode. The corresponding finger, hand and arm kinematic data was tracked using a Vicon (Oxford, UK) motion capture system.

B. Conversion to Joint Angles from Position Kinematics

The Vicon motion tracking system records the 3D position of motion tracking marker in the Cartesian coordinate space. We converted the kinematics data into 18 joint angles including the three angles of wrist (the wrist flexion-extension angle, the wrist abduction-adduction (ab-ad) angle, the wrist rotation angle), as well as the flexion-extension angle, the ab-ad angle, and the opposition angle for each of five fingers. The detailed method of converting the recorded marker positions to the joint angles can be seen in [10].

C. Motion-State-Dependent Decoding of Kinematics

There are four distinct epochs in an experimental trial. A linear dynamical system may not be able to generalize the sequence whose dynamics changes over time. Examples of such data include human motion such as running each of which exhibit complex constantly evolving dynamics. Switching linear dynamical systems (S-LDSs) are powerful models capable of describing a physical process governed by state equations that switch from time to time [17].

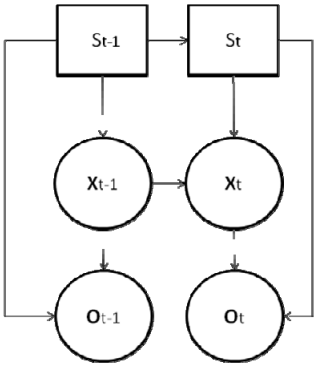

Fig. 3. Bayesian network representation of a switching linear dynamical system. Squares represent discrete states ($S_{1:N}$) while circles represent continuous states ($X_{1:N}$, $O_{1:N}$). In most cases, $S_{1:N}$ and $X_{1:N}$ are unobservable hidden states while $O_{1:N}$ are the observations. The arrows in the diagram indicate the dependency relationship between variables. In our modeling, $S_{1:N}$ have four values representing the four distinct phases in each experimental trial. $X_{1:N}$ represent the joint angles extracted from motion tracking kinematics data. $O_{1:N}$ represent single-unit firing rates of each neuron from pre-motor cortex.

S-LDSs model the discrete and continuous states (Fig. 3) which are usually hidden from observation. The state space equations of S-LDS are as follows:

$$x_{t+1} = F_t^{S_{t+1}} x_t + u_{t+1}$$

$$O_t = H_t^{S_t} x_t + z_t$$

Additionally we assume that the state noise $u_t \sim N\left(0, \ \Sigma^{S_t}{}_u\right)$ and measurement noise $z_t \sim N\left(0, \ \Sigma^{S_t}{}_z\right)$.

In our model, each phase is modeled as a discrete system state S. Each 18-dimension joint angle vector per 5 ms is modeled a continuous system state X, and the spike firing rate of all neurons in pre-motor cortex during the previous 5 ms is modeled as the observation O. Different from most problems using S-LDS models, the transitions between the discrete states $S_{1:N}$ are deterministic and observable in the current experimental setting. The continuous states $X_{1:N}$ are also available during the learning period. Therefore, there was no need for using probabilistic inference methods of S-LDS. Instead, we trained a Kalman filter [13, 17] for each phase of the experiments. In order to get robust parameter estimation, we tied the parameters $\left\{H(i), F(i), \Sigma^{S_t}{}_u(i), \Sigma^{S_t}{}_z(i)\right\}$ where $i = 1, 2 \ldots N$ are the frames in each experimental trial, and only estimated one set of parameters $\left\{H, F, \Sigma^{S_t}{}_u, \Sigma^{S_t}{}_z\right\}$ for each Kalman filter corresponding to each epoch. So the state space equations of the S-LDS are modified as follows:

$$x_{t+1} = F^{S_{t+1}} x_t + u^{S_t}$$

$$O_t = H^{S_t} x_t + z^{S_t}$$

where the state noise $u \sim N\left(0, \ \Sigma^{S_t}{}_u\right)$ and measurement noise $z \sim N\left(0, \ \Sigma^{S_t}{}_z\right)$. Note all the S-LDS parameters only change with phases of the experiments instead of changing from frame to frame. The decoding algorithm of S-LDSs

follows the Kalman filter algorithm, which includes two steps, namely, prediction and update.

1) Prediction

Based on the prior state estimate $\hat{X}_{t-1}$ at time t $\left(\hat{X}_{t-1} \in R^{18}\right)$, we predict $\hat{X}_t$ using the system transition model corresponding to each experimental phase.

$$\hat{X}_t = F^{S_t} \hat{X}_{t-1}$$

and the prior prediction error covariance $\hat{P}_t$ is predicted as

$$\hat{P}_t = F^{S_t} \hat{P}_{t-1} F^{S_t T} + \Sigma^{S_t}{}_u$$

2) Update:

The new system state, an 18-dimensional joint angle vector, $\left(\hat{X}_t \in R^{18}\right)$ is estimated at every 5 ms time step as follows:

$$\hat{X}_t = \hat{X}_t + K_t\left(O_t - H\hat{X}_t\right)$$

where the Kalman gain K_t and the posterior error covariance matrix P_t are updated as,

$$K_t = P_t H^{S_t T}\left(H^{S_t} P_t H^{S_t T} + \Sigma^{S_t}{}_u\right)^{-1}$$

$$P_t = \left(1 - K_t H^{S_t}\right) P_t$$

Mutually exclusive feature sets were used for training (80%) and testing (20%) for each task. All the results here were averaged via 5-fold cross-validation.

D. Virtual World in MSMS

We simulated the real-world experimental setup using a virtual environment created by Musculoskeletal Modeling Software (MSMS) [9] which was developed by the University of Southern California (Fig. 1A). MSMS includes detailed models for the monkey's upper extremity and objects used in experiments, which can be controlled via specifying the individual positions or joint angles in the upper extremity. The virtual environment in MSMS is programmable and can be modified to different experimental settings easily.

III. Experimental Results

The S-LDS decoder was trained offline in Matlab 7.13 using recorded neural signals from pre-motor cortex (n=43) and corresponding motion capture data of the monkey. Table I shows the mean correlation coefficients for continuous prediction of finger, hand, and arm kinematics during the reach-to-grasp tasks. As is seen from the table, neuronal activity from the pre-motor cortex predicted the kinematics of all joint angles with high mean accuracy. Fig. 4 shows the reconstructed joint angles along with the real joint angles during a segment of a trial, the reconstructed joint angles match with the real joint angles with high accuracy.

Our decoding results using S-LDS with neural signals from pre-motor cortex are better than the decoding result using a single Kalman filter with neural signals from motor cortex (mean accuracy=0.83) [10]. Assuming that PM ensembles and M1 ensembles carry the same amount of information to decode the motor kinematics, our results show the S-LDS decoder can capture the constantly evolving dynamics of behavioral tasks, better than previous research approaches. It also sheds light on the nature of motor control mechanisms used by primates during instructed tasks: at different phases of the experiments, primates may adopt different motor control mechanisms to accomplish the instructed tasks.

Both the actual joint angles recorded from real-world experiments and the decoded joint angles from the S-LDSs were then transmitted into the virtual environment in the MSMS, and the experimental trials were replicated with animation. Fig. 5 shows the reconstructed upper extremity (blue shadow arm) overlaid with the actual upper extremity (gray solid arm) as the monkey performed different behavioral tasks. As shown in our simulation results, the decoded output closely resembles the original movements of the upper extremity, especially the subtle movements of the hand and fingers during different behavioral tasks.

TABLE I
DECODING ACCURACY (CORRELATION COEFFICIENT) FOR 18-JOINT ANGLES IN FOUR DIFFERENT REACH-TO-GRASP TASKS

	PUSH	MALLET	SPHERE	PULL
Wrist	0.897	0.878	0.898	0.893
Thumb	0.899	0.884	0.898	0.896
Index	0.890	0.875	0.827	0.822
Middle	0.893	0.868	0.870	0.857
Ring	0.893	0.886	0.891	0.885
Pinky	0.891	0.877	0.881	0.894
Total	0.890	0.868	0.885	0.877

Note that the correlation values presented in the table above were averaged across all trials of each task.

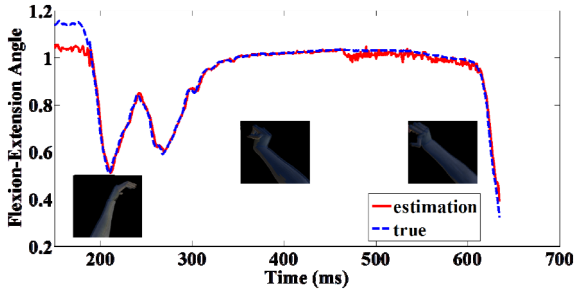

Fig. 4. Reconstruction of the flexion-extension angle of the middle finger (in radians), one of the 18 joint angles, from recorded neuronal ensembles from PMd and PMv in the task of pushing a button. Actual joint angles (solid, red) are decoded from cortical ensembles from PMd and PMv (dotted, blue). The corresponding hand gestures at 200 ms, 400 ms and 600 ms are shown. The initial discrepancy between the true curve and the estimated one is because that we intentionally add disturbance into the decoder to see how well it can handle noise.

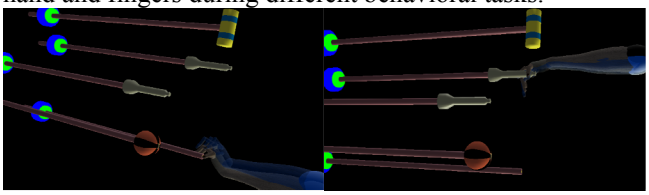

Fig. 5 Both the actual kinematics recorded during real-world experiments and the decoded joint angles were transmitted into the virtual environment in MSMS to simulate the real experiments. The example movements are pushing a button and grasping a cylinder.

IV. Conclusion

This work has two main contributions. First, this work demonstrates that it is possible to decode kinematics of the fingers, hand and arm with high mean accuracy using the pre-motor cortex neural ensembles. Related Studies showed that when monkeys performed highly similar reaches under tight behavioral control, which is true in our experimental design, the neural activity in PMd was predominantly stable over time in all measured properties such as firing rate, directional tuning, and contribution to a decoding model that predicted kinematics from PMd neuronal ensembles [16]. The changes in PMd neural activity were mainly correlated with the behavioral changes. There is, thus, a stable relationship between the PM neural activity and observed behavior kinematics [16]. Our findings about the high decoding capability of PM ensembles has significant implications for the design of neural prosthetic systems because it suggests that a general purpose BMI can employ multiple cortical areas for motor control.

We are also interested in learning dynamic models from the synchronously recorded neural activity and motion tracking kinematics data. By mapping discrete hidden states to piecewise linear dynamical system models, the S-LDS framework potentially has greater modeling power than a single Kalman filter as what most previous research used. In traditional S-LDS settings, the exact inference is usually intractable and approximate inference algorithms are developed for S-LDS learning. In this paper we exploit the uniqueness in the current decoding problem, and present a principled framework for S-LDS learning and apply it to motion kinematics decoding from neural ensembles. The key difference between the current problem setting and previous S-LDS problem settings is that the discrete state $S_{1:N}$ and the continuous states $X_{1:N}$ are both observable during learning period of the current setting, which greatly simplifies the inference procedure. Multiple Kalman filters were trained as linear dynamical systems, so the resulting decoding algorithm provides a principled linear dynamical system model of motor-cortical coding, and is easy to implement and can be applied to real-time decoding systems. Our decoding results confirm that S-LDS decoder has more descriptive power than a single Kalman filter with tied parameters for motor-cortical decoding tasks. S-LDS models can potentially be widely applied in general neural decoding for motor kinematics.

The switching between the discrete states in S-LDS is controlled by the experiment process in this work. However, in real-life applications, the switching should be automatically controlled via decoding neural activities from multiple brain areas. Our group has also investigated decoding the switching of cognitive states using neural recordings from premotor and somatosensory cortex [18], and our results suggest that it is feasible to achieve high automation in cognitive state decoding.

Our results demonstrate that motion-state-dependent decoding may enable adaptive decoding with high accuracy using neural ensembles in PMv and PMd. This is a critical step towards the development of a BMI for adaptive neural control of a clinically viable prosthesis.

Acknowledgment

The authors acknowledge Dr. Adam G. Davidson for assisting with the experimental studies, Drs. Vikram Aggarwal and Mohsen Mollazadeh for providing interpretation of experimental datasets.

References

[1] D. M. Taylor, *et al*., "Direct cortical control of 3D neuroprosthetic devices," *Science*, vol. 296, pp. 1829-32, Jun 7 2002.

[2] M. D. Serruya, *et al*., "Instant neural control of a movement signal," *Nature*, vol. 416, pp. 141-2, Mar 14 2002.

[3] L. R. Hochberg, *et al.*, "Neuronal ensemble control of prosthetic devices by a human with tetraplegia," *Nature*, vol. 442, Jul 13 2006

[4] J. M. Carmena, *et al*., "Learning to control a brain-machine interface for reaching and grasping by primates," *PLosS Biol*, vol. 1, Nov 2003.

[5] D. M. Taylor *et al.*, "Information conveyed through brain-control: cursor versus robot, " *IEEE Trans Neural Syst Rehabil Eng*, vol. 11, pp. 195-9, Jun 2003.

[6] P. R. Kennedy, R. A. Bakay, M. M. Moore, K. Adams, and J. Goldwaithe. "Direct control of a computer from the human central nervous system," *IEEE Trans Rehabil Eng*, vol. 8, pp. 198 –202, 2000.

[7] M. Velliste, S. Perel , M. C. Spalding , A. S. Whitford & A. B. Schwartz, "Cortical control of a prosthetic arm for self-feeding," *Nature*, vol. 453, pp. 1098-101, Jun 19 2008.

[8] V. Aggarwal, S. Acharya, F. Tenore, H. Shin, R. Etienne-Cummings, M. H. Schieber, N. V. Thakor, "Asynchronous decoding of dexterous finger movements using M1 neurons, " *IEEE Trans Neural Syst Rehabil Eng*, vol. 16, pp. 3-14, Feb 2008.

[9] V. Aggarwal, G. Singhal, J. He, M. H. Schieber, N. V. Thakor, "Towards closed-loop decoding of dexterous hand movements using a Virtual Integration Environment," *Conf Proc IEEE Eng Med Biol Soc*, pp. 388-91, 2011.

[10] V. Aggarwal, M. Kerr, A. G. Davidson, R. Davoodi, G. E. Loeb, M. H. Schieber, N. V. Thakor, "Cortical control of reach and grasp kinematics in a virtual environment using musculoskeletal modeling software," *Conf Proc IEEE Eng Med Biol Soc*, pp. 1703-06, 2008.

[11] V. Aggarwal, M. Mollazadeh, A. G. Davidson, M. H. Schieber, and N. V. Thakor. "State-space decoding of hand and finger kinematics using neurons ensemble and LFP activity during a reach-to-grasp task", submitted for publication.

[12] C. E. Vargas-Irwin, G. Shakhnarovich, P. Yadollahpour, J. M. K. Mislow, M. J. Black, and J. P. Donoghue, "Decoding complete reach and grasp actions from local primary motor cortex populations," *J Neurosci*, vol. 30, pp. 9659-69, Jul 21 2010.

[13] W. Wu, Y. Gao, E. Bienenstock, J. P. Donoghue, M. J. Black, "Bayesian population decoding of motor cortical activity using a Kalman Filter," *Neural Comput*, vol. 18, Jan 2006.

[14] N. Hatsopoulos, J. Joshi, and J. G. O'Leary. "Decoding continuous and discrete motor behaviors using motor and premotor cortical ensembles," *J Neurophysiolo*, vol. 92, pp. 1165-74, 2204.

[15] A. K Bansal, C. E Vargas-Irwin, W. Truccolo, J. P Donoghue, "Relationships among low-frequency local field potentials, spiking activity, and 3-D reach and grasp kinematics in primary motor and ventral premotor cortices," *J Neurophysiolo*, vol. 106, pp. 1599, 2011.

[16] C. A. Chestek, A. P. Batista, G. Santhanam, B. M. Yu, A. Afshar, J. P. Cunningham, V. Gilja, S. I. Ryu, M. M. Churchland, K. V. Shenoy, "Single-Neuron Stability during Repeated Reaching in Macaque Premotor Cortex," *J Neurosci*, vol. 27, pp. 10742-50, Oct 3, 2007.

[17] Greg Welch, Gary Bishop, "An Introduction to the Kalman Filter," *In Practice*, vol. 7(1), pp. 1-16. 2006.

[18] X. Kang, S. Sarma, M. Schieber, and N. V. Thakor, "Hidden Markov model based state decoding in primate reach-to-grasp tasks using premotor cortical ensembles", *IEEE Trans on Bio Medi Eng*. Under Review. 2012.